HOKKAIDO UNIVERSITY

Title	Extension of Traveling-Wave Parametric Amplifier Theory
Author(s)	Sakuraba, Ichiro
Citation	Memoirs of the Faculty of Engineering, Hokkaido University, 11(4), 435-446
Issue Date	1963-03
Doc URL	https://hdl.handle.net/2115/37840
Type	departmental bulletin paper
File Information	11(4)_435-446.pdf



Hokkaido University Collection of Scholarly and Academic Papers : HUSCAP

Extension of Traveling-Wave Parametric Amplifier Theory*

Ichiro SAKURABA

Department of Electronic Engineering

Contents

Page

Summary 435
1. Introduction 435
2. Analysis 436
3. Power gain 442
4. Noise figure 443
5. Conclusions 444
References 445
Appendix 445
Acknowledgment 446

Summary

This paper presents an analysis of the traveling-wave parametric amplifier in which the signal, the first upper and lower sidebands around the fundamental pump frequency and the second lower sideband around the second pump harmonic are coupled together. The dervation of the equations was based on the usual traveling-wave parametric amplifier model of Tien and Suhl. The theoritical results are much closer to the measurements than were the results of the work presented by previous workers.

1. Introduction

A great deal of attention currently is being given to increasing the bandwidth capabilities of parametric amplifiers using ferromagnetic materials, junction diodes and space-charge waves by application of traveling-wave circuit techniques. In many respects, this situation is reminiscent of the evolution of broad band traveling-wave tubes from Klystron amplifiers employing resonant cavities. The analyses[1~5] of the traveling-wave parametric amplifier were previously investigated using a model in which coupling between only the first lower sideband and the signal was considered. However, the basic principles of parametric operation generate many sidebands at different frequencies. T. Makimoto[6] explains a brief effect of including multi-frequency coupling on the

* Received September 29, 1962.

amplification. J. S. Cook and W. H. Louisell[7] show the qualitative effect on the performance. S. Saito[8] investigated numerical calculations of the effect of the higher harmonic components on the amplification and noise figure of the longitudinal-beam type of parametric amplifier after some modifications of Haus' formula, but the result is restricted to the case where the signal approximately equals the first lower sideband. H. Sobol[9] presented an analysis of the longitudinal-beam parametric amplifier in which coupling is allowed between the signal, the lower and upper sidebands around the fundamental pump frequency, but his calculations are for the degenerate case in which the signal equals the lower sideband, and he did not analyse the noise figure. In the designing of slow wave circuits or loaded transmission lines, it is important that the effect of including higher idler components on the power gain and the noise fignre be given by a general formula. Then it may be shown that deterioration of the performance can easily be given after some modifications[10~12] of Tien's analysis.

2. Analysis

The analysis in which more idler frequencies are taken into account is given under the following assumptions;

1) The signal (ω_1) and all its higher harmonics (ω_2, $\omega_3 \cdots$) are so small that the small signal theory can be applied.

2) The pumping wave (ω) with a propagation constant, β, has a power level substantially larger than that of the signal and its harmonics, and is so small that the second order coupling between the signal and the pumping waves can be neglected.

3) The signal (ω_1), the first lower sideband wave or idler (ω_2), the first upper sideband wave (ω_3), and the second lower sideband wave (ω_4) are carried by four propagating circuits. The relation of these frequencies is shown in Fig. 1.

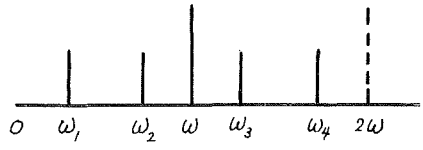


Fig. 1. Relation of pump, signal and idler frequencies. The frequencies satisfy $\omega = \omega_1 + \omega_2$, $\omega = \omega_3 - \omega_1$ and $\omega_4 = 2\omega - \omega_1$.

4) Four waves are coupled through a distributed inductance

$$L_{(z,t)} = L_{(z,t)}e^{j\omega t} + L^*_{(z,t)}e^{-j\omega t} = L\left[e^{j(\omega t - \beta z)} + e^{-j(\omega t - \beta z)}\right] \qquad (1)$$

Here $*$ denotes the complex conjugate, t is time and z is distance.

A variable reacter such as the one shown in equation (1), may be obtained by feeding a pumping wave to a nonlinear medium in such a way that the equivalent permeability or dielectric of the medium varies with the intensity of the pumping field. The medium may be a ferrite sample, an electron beam or a series of junction diodes. The pumping wave may be supported by a separate propagation structure or by one of the circuits which carry the ω_1, ω_2, ω_3 and ω_4 waves.

5) The phase and group velocities of all waves face the same direction.

6) The conditions on the phases are

$$\beta_2 = \beta - \beta_1 , \quad \beta_3 = \beta + \beta_1 , \quad \beta_4 = 2\beta - \beta_1 ,$$

where β_1, β_2, β_3 and β_4 are the phase constants of ω_1, ω_2, ω_3 and ω_4, respectively.

7) The transmission loss is small and may be neglected.

8) After dividing the propagating circuit into small sections, each section of the circuit is represented by a filter type network as shown in Fig. 2.

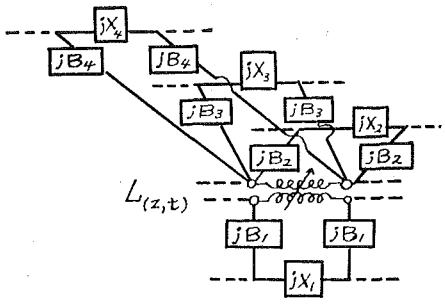


Fig. 2. An equivalent circuit of a traveling-wave parametric circuit with higher idler frequencies.

If the i circuit has a series reactance jX_i and a shunt susceptance jB, the phase constant and the charactristic impedance of the propagating circuit are,

$$\beta_i = (X_i B_i)^{1/2}, \quad Z_{0i} = (X_i/B_i)^{1/2}, \quad i = 1, 2, 3, 4 . \tag{2}$$

If $V_{i(z,t)}$ and $I_{i(z,t)}$ are the voltage and current of the i circuit, the differential equations for line are as follows;

$$\left.\begin{aligned} \frac{\partial V_{1(z,t)}}{\partial z} &= -jX_1 I_{1(z,t)} - \frac{\partial}{\partial t}\left\{L_{(z,t)}[I_{2(z,t)} + I_{3(z,t)} + I_{4(z,t)}]\right\} \\ \frac{\partial I_{1(z,t)}}{\partial z} &= -jB_1 V_{1(z,t)} \\ \frac{\partial V_{2(z,t)}}{\partial z} &= -jX_2 I_{2(z,t)} - \frac{\partial}{\partial t}\left\{L_{(z,t)}[I_{1(z,t)} + I_{3(z,t)} + I_{4(z,t)}]\right\} \end{aligned}\right\} \tag{3}$$

$$\left.\begin{aligned}
\frac{\partial I_{2(z,t)}}{\partial z} &= -jB_2 V_{2(z,t)} \\
\frac{\partial V_{3(z,t)}}{\partial z} &= -jX_3 I_{3(z,t)} - \frac{\partial}{\partial t}\left\{L_{(z,t)}[I_{1(z,t)}+I_{2(z,t)}+I_{4(z,t)}]\right\} \\
\frac{\partial I_{3(z,t)}}{\partial z} &= -jB_3 V_{3(z,t)} \\
\frac{\partial V_{4(z,t)}}{\partial z} &= -jX_4 I_{4(z,t)} - \frac{\partial}{\partial t}\left\{L_{(z,t)}[I_{1(z,t)}+I_{2(z,t)}+I_{3(z,t)}]\right\} \\
\frac{\partial I_{4(z,t)}}{\partial z} &= -jB_4 V_{4(z,t)}
\end{aligned}\right\}$$

Combination of the first equation with the second, the third with the fourth and the fifth with the sixth yields

$$\left.\begin{aligned}
\frac{\partial^2 I_{1(z,t)}}{\partial z^2} &= -X_1 B_1 I_{1(z,t)} + jB_1 \frac{\partial}{\partial t}\left\{L_{(z,t)}[I_{2(z,t)}+I_{3(z,t)}+I_{4(z,t)}]\right\} \\
\frac{\partial^2 I_{2(z,t)}}{\partial z^2} &= -X_2 B_2 I_{2(z,t)} + jB_2 \frac{\partial}{\partial t}\left\{L_{(z,t)}[I_{1(z,t)}+I_{3(z,t)}+I_{4(z,t)}]\right\} \\
\frac{\partial^2 I_{3(z,t)}}{\partial z^2} &= -X_3 B_3 I_{3(z,t)} + jB_3 \frac{\partial}{\partial t}\left\{L_{(z,t)}[I_{1(z,t)}+I_{2(z,t)}+I_{4(z,t)}]\right\} \\
\frac{\partial^2 I_{4(z,t)}}{\partial z^2} &= -X_4 B_4 I_{4(z,t)} + jB_4 \frac{\partial}{\partial t}\left\{L_{(z,t)}[I_{1(z,t)}+I_{2(z,t)}+I_{3(z,t)}]\right\}
\end{aligned}\right\} \quad (4)$$

These are familiar equations except for the coupling terms. We shall assume the coupling terms to be small, compared with the other terms in the equations so that calculation can be made by the perturbation method. We should point out that equation (4) is derived by assuming $I_{i(z,t)}$ to be in the form $A_{i(z)}$ exp $j\omega_i t$, if $I_{i(z,t)}=A^*_{i(z)}$ exp $(-j\omega t)$ the sign of the coupling term in equation (4) is reversed. In the following assumptions, let the conditions on the phase constants and frequencies be

$$\omega_2=\omega-\omega_1\,, \qquad \omega_3=\omega+\omega_1\,, \qquad \omega_4=2\omega-\omega_1\,, \tag{5}$$

$$\beta_2=\beta-\beta_1\,, \qquad \beta_3=\beta+\beta_1\,, \qquad \beta_4=2\beta-\beta_1\,. \tag{6}$$

The complete solution of equation (4) must be the sum of coupled pairs. Here for simplification, we shall analyse the next pair only. Put

$$\begin{aligned}
I_{1(z,t)} &= A_{1(z)}\, e^{j(\omega_1 t-\beta_1 z)} \\
I^*_{2(z,t)} &= A^*_{2(z)}\, e^{-j(\omega_2 t-\beta_2 z)} \\
I_{3(z,t)} &= A_{3(z)}\, e^{j(\omega_3 t-\beta_2 z)} \\
I^*_{4(z,t)} &= A^*_{4(z)}\, e^{-j(\omega_4 t-\beta_4 z)}
\end{aligned}$$

From the following lines of approach similar to those described in the text of Tien and Suhl[1], we obtain a set of equations

$$\left.\begin{aligned}
\frac{\partial A_{1(z)}}{\partial z} &= -j\frac{1}{2}\frac{\omega_1 B_1 L}{\beta_1}\left[A^*_{2(z)}+A_{3(z)}\right]\\
\frac{\partial A^*_{2(z)}}{\partial z} &= j\frac{1}{2}\frac{\omega_2 B_2 L}{\beta_2}\left[A_{1(z)}+A^*_{4(z)}\right]\\
\frac{\partial A_{3(z)}}{\partial z} &= -j\frac{1}{2}\frac{\omega_3 B_3 L}{\beta_3}A_{1(z)}\\
\frac{\partial A^*_{4(z)}}{\partial z} &= j\frac{1}{2}\frac{\omega_4 B_4 L}{\beta_4}A^*_{2(z)}
\end{aligned}\right\} \qquad (7)$$

It can easily be shown that equation (7) satisfies the Manley-Rowe power relationship, as shown in Appendix. Equation (7) may be reduced in the form

$$\frac{\partial^4 A_{1(z)}}{\partial z^4}+\frac{L^2}{4}\left(\frac{\omega_1\omega_3}{Z_{02}Z_{03}}+\frac{\omega_2\omega_4}{Z_{02}Z_{04}}-\frac{\omega_1\omega_2}{Z_{01}Z_{02}}\right)\frac{\partial^2 A_{1(z)}}{\partial z^2}+\frac{L^4}{16}\frac{\omega_1\omega_2\omega_3\omega_4}{Z_{01}Z_{02}Z_{03}Z_{04}}A_{1(z)}=0 \qquad (8)$$

For understanding the effect of higher harmonics, it is assumed that

$$Z_{01}Z_{03}=Z_{02}Z_{04}=Z_{01}Z_{02} \qquad (9)$$

where Z_{01}, Z_{02}, Z_{03} and Z_{04} are the characteristic impedances of ω_1, ω_2, ω_3 and ω_4, respectively. Thus equation (8) can be written as

$$\frac{\partial^4 A_{1(z)}}{\partial z^4}+\frac{1}{4}\xi_0^2(3n^2-3n+2)\frac{\partial^2 A_{1(z)}}{\partial z^2}+\frac{1}{16}\xi_0^2(1-n^2)(2-n)nA_{1(z)}=0 \qquad (10)$$

where $\omega^2L^2/Z_{01}Z_{02}=\xi_0^2$, $\omega_1/\omega=n$, $0.5\geqq n>0$. Then the solution of equation (10) is

$$A_{1(z)}=a_1e^{\delta_1\xi_0 z}+b_1e^{\delta_2\xi_0 z}+c_1e^{\delta_3\xi_0 z}+d_1e^{\delta_4\xi_0 z} \qquad (11)$$

δ can be determined from equation (12),

$$\delta^4+\frac{1}{4}(3n^2-3n+2)\delta^2+\frac{1}{16}(1-n^2)(2-n)n=0 \qquad (12)$$

In equation (11), a_1, b_1, c_1 and d_1 are arbitrary constants. In dealing with equation (12), let

$$\delta=x+jy \qquad (13)$$

From equation (11), we see that, if $x>0$, the wave increases as it travels,

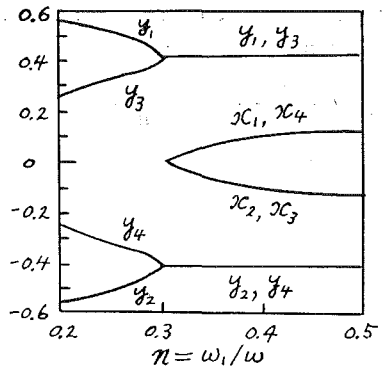


Fig. 3. The x's and y's for waves versus the ratio of the signal frequency to the fundamental pump frequency. Here the four waves vary with distance as exp $(-j\beta+\delta\xi_0)z$ where $\delta=x+jy$.

and if $x<0$, the wave decreases as it travels, and y means the difference of phase constant after coupling. Curves of δ are shown in Fig. 3. Increasing waves are found for $0.5\geqq n>0.303$. Maximum x occurs under the degenerated case in which $n=0.5$. This coinsides with the results by Saito[8] and Sobol[9]. For $n<0.303$, it is noted that all the coupled waves are neither growing nor attenuating.

Finally from equations (7) and (11) the following equations may be led

$$\left.\begin{aligned} I_{1(z,t)} &= e^{j(\omega_1 t-\beta_1 z)}\left(a_1 e^{\delta_1\xi_0 z}+b_1 e^{-\delta_1\xi_0 z}+c_1 e^{\delta_3\xi_0 z}+d_1 e^{-\delta_3\xi_0 z}\right)\\ I^*_{2(z,t)} &= e^{-j(\omega_2 t-\beta_2 z)}\left[M_2(a_1 e^{\delta_1\xi_0 z}-b_1 e^{-\delta_1\xi_0 z})+N_2(c_1 e^{\delta_3\xi_0 z}-d_1 e^{-\delta_3\xi_0 z})\right]\\ I_{3(z,t)} &= e^{j(\omega_3 t-\beta_3 z)}\left[M_3(a_1 e^{\delta_1\xi_0 z}-b_1 e^{-\delta_1\xi_0 z})+N_3(c_1 e^{\delta_3\xi_0 z}-d_1 e^{-\delta_3\xi_0 z})\right]\\ I^*_{4(z,t)} &= e^{-j(\omega_4 t-\beta_4 z)}\left[M_4(a_1 e^{\delta_1\xi_0 z}+b_1 e^{-\delta_1\xi_0 z})+N_4(c_1 e^{\delta_3\xi_0 z}+d_1 e^{-\delta_3\xi_0 z})\right] \end{aligned}\right\} \tag{14}$$

where

$$M_2=\left(\frac{\gamma_3}{\delta_1\xi_0}-\frac{\delta_1\xi_0}{\gamma_1}\right)\quad M_3=-\gamma_3/\delta_1\xi_0.\quad M_4=\left(\frac{\gamma_3}{\delta_1^2\xi_0^2}-\frac{1}{\gamma_1}\right)\gamma_4$$

$$N_2=\left(\frac{\gamma_3}{\delta_3\xi_0}-\frac{\delta_3\xi_0}{\gamma_1}\right)\quad N_3=-\gamma_3/\delta_3\xi_0.\quad N_4=\left(\frac{\gamma_3}{\delta_3^2\xi_0^2}-\frac{1}{\gamma_2}\right)\gamma_4 \tag{15}$$

$$\gamma_i=\frac{j}{2}\frac{\omega_i B_i L}{\beta_i}$$

In the following case

$$I_{1(0,t)}=ae^{j(\omega_1 t+\theta)},\qquad I^*_{2(0,t)}=I_{3(0,t)}=I^*_{4(0,t)}=0\,. \tag{16}$$

For $0.5\geqq n>0.303$, equation (14) becomes

$$\left.\begin{aligned}
I_{1(z,t)} &= e^{j(\omega_1 t-\beta_1 z+\theta)}\frac{a}{M_4^*-M_4}\left[M_4^*\cosh(\delta_1\xi_0 z)-M_4\cosh(\delta_1^*\xi_0 z)\right]\\
I_{2(z,t)}^* &= e^{-j(\omega_2 t-\beta_2 z-\theta)}\frac{a}{M_4^*-M_4}\left[M_2M_4^*\sinh(\delta_1\xi_0 z)+M_2^*M_4\sinh(\delta_1^*\xi_0 z)\right]\\
I_{3(z,t)} &= e^{j(\omega_3 t-\beta_3 z+\theta)}\frac{a}{M_4^*-M_4}\left[M_2M_4^*\sinh(\delta_1\xi_0 z)+M_3^*M_4\sinh(\delta_1^*\xi_0 z)\right]\\
I_{4(z,t)}^* &= e^{-j(\omega_4 t-\beta_4 z-\theta)}a\frac{M_4M_4^*}{M_4^*-M_4}\left[\cosh(\delta_1\xi_0 z)-\cosh(\delta_1^*\xi_0 z)\right]
\end{aligned}\right\}\quad(17)$$

where

$$N_2=M_2^*,\qquad N_3=M_3^*,\qquad N_4=M_4^*.\qquad(18)$$

The amplitudes of $I_{1(z,t)}$, $I_{2(z,t)}^*$, $I_{3(z,t)}$ and $I_{4(z,t)}^*$ are plotted in Fig. 4, which should be compared with coupling only between the signal and its lower

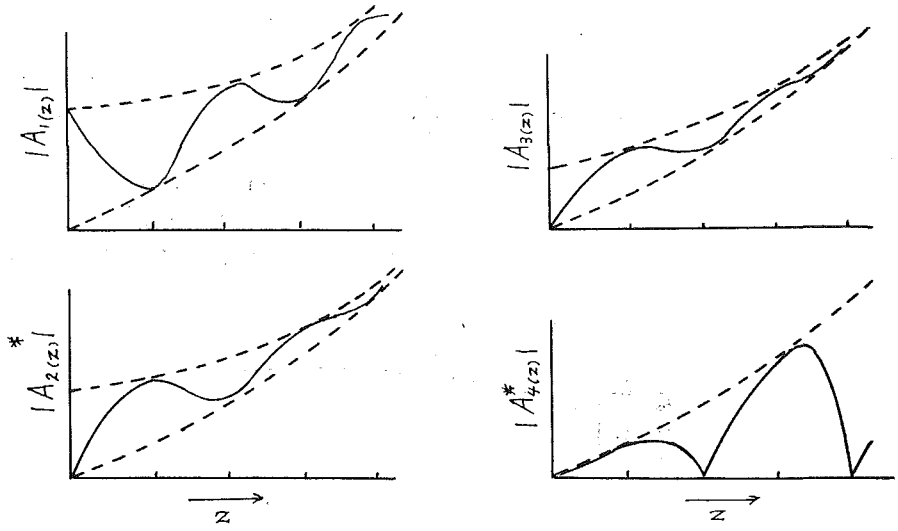


Fig. 4. The amplitudes of the ω_1, ω_2, ω_3 and ω_4 waves plotted along the direction of propagation.

sideband. It is noted that these forms resemble amplitude-modulated increasing waves and the amplitude of $I_{4(z,t)}^*$ is zero at $y_1\xi_0 z=0, \pi, 2\pi, \cdots$.

For $n<0.303$, we have

$$\left.\begin{aligned}
I_{1(z,t)} &= e^{j(\omega_1 t-\beta_1 z+\theta)}\frac{a}{N_4-M_4}\left[N_4\cos(y_1\xi_0 z)-M_4\cos(y_1\xi_0 z)\right]\\
I_{2(z,t)}^* &= e^{-j(\omega_2 t-\beta_2 z-\theta)}\frac{ja}{N_4-M_4}\left[M_3N_4\sin(y_1\xi_0 z)-M_4N_2\sin(y_1\xi_0 z)\right]
\end{aligned}\right\}\quad(19)$$

$$I_{3(z,t)} = e^{j(\omega_3 t-\beta_3 z+\theta)}\frac{ja}{N_4-M_4}\left[M_3N_4\sin(y_1\xi_0 z)-M_4N_3\sin(y_3\xi_0 z)\right]$$
$$I^*_{4(z,t)} = e^{-j(\omega_4 t-\beta_4 z-\theta)}\frac{M_4N_4}{N_4-M_4}\left[\cos(y_1\xi_0 z)-\cos(y_3\xi_0 z)\right]$$

3. Power Gain

It is assumed that a signal is applied at frequency ω_1. From equation (17) it follows that the average power transmitted down the line exponentially increases and that gains can be achieved. The power gain in decibels in a length s is given by

$$\text{gain (db)} = 20\log(\cosh x_1\xi_0 s).$$

If the amplifier is long enough so that $x_1\xi_0 s \gg 1$, the gain can be expressed approximately as

$$\text{gain (db)} \fallingdotseq 8.68\, x_1\xi_0 s - 6 \text{ db} \tag{20}$$

so that the maximum gain occurs when $n=0.5$. Here the second term, -6, is a loss relating power associated with the growing wave to the total applied signal. The power gain in various conditions described above is plotted in Fig. 5. The curve (a) of Fig. 5 shows the gain when the signal, the idler, the first upper sideband and the second lower sideband are coupled together. For coupling only between the signal and the idler, the power gain is given

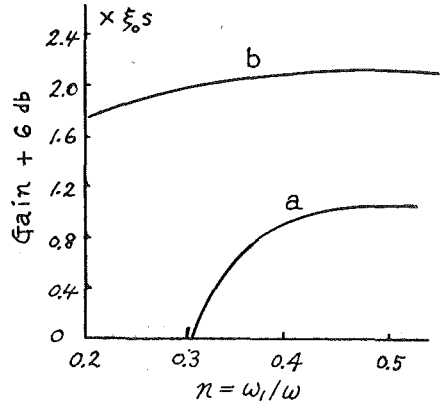


Fig. 5. Power gain of a traveling-wave parametric amplifier versus the ratio $n=\omega_1/\omega$, a) ω_1, ω_2, ω_3 and ω_4 waves are coupled together; b) coupling only between ω_1 and ω_2. At $n=0.5$, the effect of including the multi-frequency coupling is to reduce the gain to one half the db value predicted by earlier works.

by the curves (b) of Fig. 5, as shown by Tien[3]. From the calculations described above, the effect of including the multi-frequency coupling is to reduce the gain to one half the db value predicted in earlier analyses. These theoritical analyses are much closer to the measurements than were the results of the earlier workers[1~5].

4. Noise Figure

The primary advantage of parametric amplifiers is their extremely low noise capabilities. A discussion of the noise figure of including the multi-frequency coupling will now be presented.

It is assumed that the input is connected to a matched signal source at $T_1=290°K$ at frequency ω_1. Further assume that at ω_2, ω_3 and ω_4, the input ends are matched passive impedances at temperature T_2, T_3 and T_4, respectively, and the output ends are matched to a load at temperature T_s. This is shown

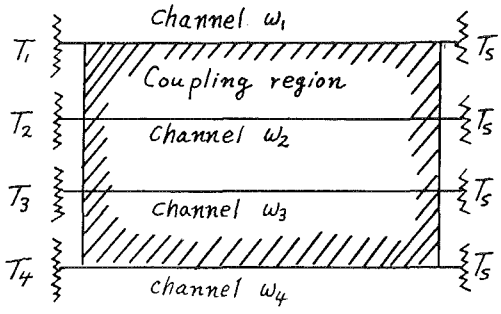


Fig. 6. Schematic representation of four channels for noise and signal in a traveling-wave parametric amplifier. The input of ω_1, ω_2, ω_3 and ω_4 channels are in matched impedances at respective temperature T_1, T_2, T_3 and T_4, and the outputs of their channels are terminated in matched impedances at temperature T_s.

schematically in Fig. 6. The pumping wave, signal, idler, the first upper and the second lower sidebands satisfy equations (5) and (6), so that the noise inputs, kT_1B, kT_2B, kT_3B and kT_4B of ω_1, ω_2, ω_3 and ω_4 circuits, respectively, give a noise output

$$kT_1B+\frac{\omega_1}{\omega_2}kT_2B(G-1)+\frac{\omega_1}{\omega_3}kT_3B(G-1)+\frac{\omega_1}{\omega_4}kT_4B(G-1) \quad (21)$$

at $z=s$ of the circuit, where $y_1\xi_0 s \neq n\pi$, $(n=1, 2, 3, \cdots)$. If $y_1\xi_0 s=n\pi$, the fourth term becomes zero.

If a signal, $S_{in(\omega_1)}$, is introduced at ω_1 only, then from the definition of

gain, $S_{out(\omega_1)}=G\cdot S_{in(\omega_1)}$ and equation (21), the noise figure, F, is

$$F=1+\frac{\omega_1}{\omega_2}\frac{T_2}{T_1}\frac{G-1}{G}+\frac{\omega_1}{\omega_3}\frac{T_3}{T_1}\frac{G-1}{G}+\frac{\omega_1}{\omega_4}\frac{T_4}{T_1}\frac{G-1}{G} \tag{22}$$

If $G\gg 1$, equation (22) becomes

$$F\fallingdotseq 1+\frac{\omega_1 T_2}{\omega_2 T_1}+\frac{\omega_1 T_3}{\omega_3 T_1}+\frac{\omega_1 T_4}{\omega_4 T_1} \tag{23}$$

When $T_1=T_2=T_3=T_4$, the noise figure is

$$F=1+\frac{n}{1-n}+\frac{n}{1+n}+\frac{n}{2-n} \tag{24}$$

Now, $\omega_1=\omega_2$, it is seen that the noise figure is 4.3 db, which is larger than that of the coupling only between the signal and idler by 1.3 db. This relation is shown in Fig. 7. The curve (a) of Fig. 7 gives the noise figure

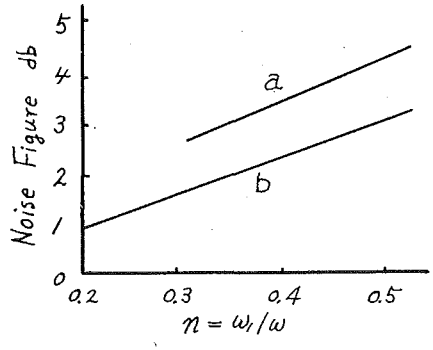


Fig. 7. Noise figure versus the ratio $n=\omega_1/\omega$, a) ω_1, ω_1, ω_3 and ω_4 waves are coupled together; b) coupling only between ω_1 and ω_2. At $n=0.5$, the effect of higher idler frequencies is to increase the noise figure to 4.3 db.

when four waves are coupled together. In the case of coupling only between ω_1 and ω_2 the noise figure is shown by the curve (b) of Fig. 7, as given in Tien[3]. From calculations described above, the effect of including the multi-frequency is to increase the noise figure. This result agrees with the noise figure of the longitudinal-beam type computed by Saito[8], also.

5. Conclusions

An analysis in which the signal, the first upper sideband, the first lower sideband and the second lower sideband were coupled together was presented.

The calculations in this paper yielded the following interesting results:

1) The deterioration of the performance, e. g. the amplification and the noise figure, was given in a general form. The dervation of the analysis was based on the usual model of traveling-wave parametric amplifier given by Tien and Suhl.

2) The effect of including the multi-frequency was to reduce the gain to one half the db value predicted by earlier analyses and to increase the noise figure to 4.3 db.

3) The theoritical results were much closer to the measurements than were the results of the earlier workers.

References

1) P. K. Tien and H. Suhl: "A traveling-wave feromagnetic amplifier", Proc. IRE, vol. 46, pp. 700–706; April, 1958.

2) W. H. Louisell and C. F. Quate: "Parametric amprification of space charge waves", Proc. IRE, vol. 46, pp. 707–716; April, 1958.

3) P. K. Tien: "Parametric amplification and frequency mixing in propagating circuits", J. Appl. Phys, vol. 29, pp. 1347–1357; September, 1958.

4) S. Saito: "Parametric amplification of space-charge waves on a thin electron beam, "J. Inst. Elect. Commun. Engrs. Japan, vol. 43, pp. 1113–1120; November, 1958 (in Japanes).

5) B. T. Henoch: "Aspects on wide-band parametric traveling-wave amplifiers", Ericsson Technics, vol. 16, pp. 77–135; January, 1960.

6) T. Makimoto: "Parametric amplification in propagating circuits", Microwave Transmission Research Committee, Inst. Elect. Commun. Engrs. Japan; May, 1959 (in Japanese).

7) J. S. Cook and W. H. Louisell: "Fast longitudinal space-charge wave parametric amplifier", 1959 WESCON Convention Record, pt. 3, pp. 77–85.

8) S. Saito: "Effect of higher harmonic components on the performance of the traveling-wave parametric amplifier, "Proc. IRE, vol. 49, pp. 623–624; March, 1960.

9) H. Sobol: "Extension of longitudinal beam parametric amplifier theory", Proc. IRE, vol. 48, pp. 792–793; April, 1960.

10) Y. Asami and I. Sakuraba: "Gain and noise figure of traveling-wave parametric amplifiers", The Record of General Meeting, B9, Hokkaido Section of I. E. E. and I. E. C. E. of Japan; November, 1960 (in Japanese).

11) I. Sakuraba and K. Kazui: "Effect of higher idler frequencies on gain and noise figure of traveling-wave parametric amplifier, "J. Inst. Elect. Commun. Engrs. Japan, vol. 44, pp. 1803–1806; November, 1961 (in Japanese).

12) I. Sakuraba: "Extension of traveling-wave parametric amplification theory", Proc. IEEE, Vol. 51, pp. 371–372; February 1963.

Appendix

The Manley-Rowe relation under small signal and weak coupling conditions are

$$\frac{d}{dz}\left(\sum_{m=-\infty}^{\infty}\frac{a_m a_m^*}{m\omega+\omega_1}\right)dz=0$$

or

$$\sum_{m=-\infty}^{\infty}\frac{1}{m\omega+\omega_1}\left(a_m\frac{da_m^*}{dz}+a_m^*\frac{da_m}{dz}\right)dz=0 \qquad \text{(A-1)}$$

where a_m is the normal amplitude and dz is length. The relation between the mode amplitude, a_m and $A_{i(z)}$ of equation (7) is

$$a_m=A_{i(z)}\sqrt{Z_{0i}} \qquad \text{(A-2)}$$

Here Z_{0i} is the characteristic impedance of ω_i wave. The signal ($i=1$), the idler ($i=2$), the first upper sideband ($i=3$), and the second lower sideband ($i=4$) correspond to $m=0$, $m=-1$, $m=+1$ and $m=-2$, respectively. Then equation (7) becomes

$$\begin{aligned}
\frac{\partial a_0}{\partial z}&=-j\frac{1}{2}\frac{\omega_1 B_1 L}{\beta_1}\sqrt{\frac{Z_{01}}{Z_{02}Z_{03}}}\,(a_{-1}^*\sqrt{Z_{03}}+a_1\sqrt{Z_{02}})\\
\frac{\partial a_{-1}^*}{\partial z}&=j\frac{1}{2}\frac{\omega_2 B_2 L}{\beta_2}\sqrt{\frac{Z_{01}}{Z_{01}Z_{04}}}\,(a_0\sqrt{Z_{04}}+a_{-2}^*\sqrt{Z_{01}}) \qquad \text{(A-3)}\\
\frac{\partial a_1}{\partial z}&=-j\frac{1}{2}\frac{\omega_3 B_3 L}{\beta_3}\sqrt{\frac{Z_{03}}{Z_{01}}}\,a_0\\
\frac{\partial a_{-2}^*}{\partial z}&=j\frac{1}{2}\frac{\omega_4 B_4 L}{\beta_4}\sqrt{\frac{Z_{04}}{Z_{03}}}\,a_1^*
\end{aligned}$$

The equation (A-3) and its conjugate satisfy equation (A-1). Thus it was shown that equation (7) satisfies the Manley-Rowe power relationship.

Acknowledgment

The author wishes to express his sincere appreciation to Dr. Y. Asami for several illuminating discussions on this problem, and to Mr. K. Kazui for calculating the differential equations.